

LEGIBILITY NOTICE

A major purpose of the Technical Information Center is to provide the broadest dissemination possible of information contained in DOE's Research and Development Reports to business, industry, the academic community, and federal, state and local governments.

Although a small portion of this report is not reproducible, it is being made available to expedite the availability of information on the research discussed herein.

LA-UR-89-3008

DE90 000537

TITLE LANCZOS DIAGONALIZATIONS OF THE 1-D PEIERLS-HUBBARD MODEL

AUTHOR(S) Eugene Y. Loh, David K. Campbell, J. Tinka Gammel

SUBMITTED TO Proceedings of the "Workshop on Interacting Electrons in Reduced Dimensions," held Oct. 3-7, 1988, Torino, ITALY

DISCLAIMER

This report was prepared as an account of work sponsored by an agency of the United States Government. Neither the United States Government nor any agency thereof, nor any of their employees, makes any warranty, express or implied, or assumes any legal liability or responsibility for the accuracy, completeness, or usefulness of any information, apparatus, product, or process disclosed, or represents that its use would not infringe privately owned rights. Reference herein to any specific commercial product, process, or service by trade name, trademark, manufacturer, or otherwise does not necessarily constitute or imply its endorsement, recommendation, or favoring by the United States Government or any agency thereof. The views and opinions of authors expressed herein do not necessarily state or reflect those of the United States Government or any agency thereof.

The copyright of this report is the property of the United States Government. It is available to the public in accordance with the provisions of the U.S. Government's copyright policy, which is to allow others to do so for U.S. Government purposes.

The copyright of this report is the property of the publisher, directly or through its agents, as work performed under the auspices of the U.S. Department of Energy.

Los Alamos National Laboratory
Los Alamos, New Mexico 87545

LANCZOS DIAGONALIZATIONS OF THE 1-D PEIERLS-HUBBARD MODEL

E. Y. Loh, Jr., D. K. Campbell, and J. Tinka Gammel
Theoretical Division and Center for Nonlinear Studies,
Los Alamos National Laboratory, Los Alamos, NM 87545, USA

INTRODUCTION

In contrast to the relative simplicity of independent electron theories, models describing *interacting* electrons are in general difficult to treat adequately. In their full complexity, many-electron problems involving N electronic orbitals -each of which can be empty, singly occupied with an electron of either spin, or doubly occupied- require the solution of Hamiltonian matrices of size roughly 4^N by 4^N . For a given problem, symmetries and selection rules (total spin, mirror plane or electron-hole symmetry, etc.) can be used to reduce the size of the matrix, but its growth with N will still be exponential. Often one attempts to avoid this difficulty by use of approximations involving *effective* single-particle methods -such as Hartree-Fock or Fermi liquid theory- which assume that the full problem can be treated in terms of self-consistent (or renormalized) nearly independent quasi-particle states. In Hartree-Fock, for example, one assumes that the full many-body wavefunction can be written as a single Slater determinant of one-particle wave functions. Accordingly, the problem for an N orbital system involves only an N by N matrix, albeit typically with self-consistency constraints on the parameters occurring in the Hamiltonian. Unfortunately, for strongly correlated systems such mean-field approaches can break down entirely; when the physical systems involve electronic motion in reduced dimensions, where strong quantum fluctuations can dominate the physics, this breakdown is particularly likely.

Thus in studies of "interacting electrons in reduced dimensions" one is trapped between the *Scylla* of exponential growth of the number of states in any exact many-body basis and the *Charybdis* of the failure of mean-field theories to capture adequately the effects of interactions. In the present article we focus on one technique -the Lanczos method- which, at least in the case of the 1-D Peierls-Hubbard model, appears (to continue the metaphor) to allow us to sail the narrow channel between these two hazards. In contrast to Quantum Monte Carlo methods, which circumvent the exponential growth of states by statistical techniques and importance sampling, the Lanczos approach attacks this problem head on by diagonalizing the full Hamiltonian. Given the restrictions of present computers, this approach is thus limited to studying finite clusters of roughly 12-14 sites. Fortunately, in one dimension, such clusters are usually sufficient for extracting many of the properties of the infinite system provided that one makes full use of the ability to vary the boundary conditions. In this article we shall apply the Lanczos methodology^{1,2} and novel "phase randomization" tech-

niques^{3,4} to study the 1-D Peierls-Hubbard model, with particular emphasis on the optical absorption properties, including the spectrum of absorptions as a function of photon energy. Despite the discreteness of the eigenstates in our finite clusters, we are able to obtain optical spectra that, in cases where independent tests can be made, agree well with the known exact results for the infinite system. Thus we feel that this combination of techniques represents an important and viable means of studying many interesting novel materials involving strongly correlated electrons.

THF 1-D PEIERLS-HUBBARD MODEL

Over the past several years the Peierls-Hubbard Hamiltonian⁵ has emerged as an important model in which to analyze the competing (or synergetic) effects of electron-phonon (e-p) and electron-electron (e-e) interactions in a variety of quasi-one-dimensional systems, including charge transfers salts, halogen-bridged metallic chains, and conducting polymers. In the context appropriate to describe *trans*-(CH)_x (the specific material on which we shall focus here), the Hamiltonian takes the form

$$H = - \sum_{\ell} (t_0 - \alpha \delta_{\ell}) B_{\ell, \ell+1} + \frac{K}{2} \sum_{\ell} \delta_{\ell}^2 + U \sum_{\ell} n_{\ell\uparrow} n_{\ell\downarrow} + V \sum_{\ell} n_{\ell} n_{\ell+1} \quad . \quad (1)$$

We consider H defined on a ring of N sites and note that $c_{\ell\sigma}^{\dagger}(c_{\ell\sigma})$ creates (annihilates) an electron in the Wannier orbital at site ℓ , $n_{\ell\sigma} = c_{\ell\sigma}^{\dagger} c_{\ell\sigma}$, $n_{\ell} = n_{\ell\uparrow} + n_{\ell\downarrow}$, $B_{\ell, \ell+1} = \sum_{\sigma} (c_{\ell, \sigma}^{\dagger} c_{\ell+1, \sigma} + c_{\ell+1, \sigma}^{\dagger} c_{\ell, \sigma})$, t_0 is the hopping integral for the uniform (CH) ionic lattice, α is the electron-phonon coupling describing the modification of the hopping between adjacent sites due to the distortion of the underlying lattice, δ_{ℓ} is the relative displacement between the (CH) units at sites ℓ and $\ell + 1$, and K represents the cost of distorting the lattice. The Coulomb repulsions among electrons are parameterized with U and V , describing the on-site and nearest-neighbor interactions, respectively. In the limit $U = 0 = V$, eqn. (1) reduces to the familiar Su-Schrieffer-Heeger (SSH) model⁶ of *trans*-(CH)_x. Since one of our primary interests in the present study is the influence of *non-perturbative* e-e interactions, we shall typically investigate the intermediate-coupling regime by considering $U = 4t_0$, which is the full single-particle bandwidth.

For studies of the optical transitions, we shall need the current operator

$$j_{\ell, \ell+1} = i(t_0 - \alpha \delta_{\ell}) \sum_{\sigma} (c_{\ell+1, \sigma}^{\dagger} c_{\ell\sigma} - c_{\ell\sigma}^{\dagger} c_{\ell+1, \sigma}) \quad . \quad (2)$$

The Fourier transform of $j_{\ell, \ell+1}$ is

$$J_q = \frac{1}{\sqrt{N}} \sum_{\ell} e^{-iq(\ell+\frac{1}{2})} j_{\ell, \ell+1} \quad . \quad (3)$$

The optical absorption coefficient $\alpha(\omega)$ is given by

$$\alpha(\omega) = \frac{1}{\omega} \sum_m | \langle m | J_q | 0 \rangle |^2 \delta(\omega - (E_m - E_0)) \quad . \quad (4)$$

Due to the pathologies — including violation of the f sum rule and difficulties both with physical interpretation of the geometry⁷ and with phase randomization — that arise when we attempt to define $\alpha(\omega)$ on a closed N site ring for $q = 0$, we will study the smallest allowed nonzero momentum value, $q = 2\pi/N$.

THE LANCZOS METHOD

Our very large-scale diagonalization studies are made feasible by the Lanczos method^{1,2}, which in essence involves expressing the Hamiltonian in a cleverly chosen basis. One starts generating the basis set by normalizing some trial wavefunction, which we typically express in terms of real space occupations. Although there are advantages(including improved convergence) to starting with a good estimate of the ground state, we have usually chosen to start from a *random* wavefunction, subject only to the constraint that $S_z = 0$, where S_z is the z -component of the total spin. Since the Hamiltonian does not alter total spin, we are guaranteed to stay within the $S_z = 0$ manifold. Choosing a random starting wave function does not cost much extra computing time in most cases and, importantly, it statistically prevents one from picking a wavefunction with the wrong symmetry.

The Lanczos procedure is to generate the matrix elements of the Hamiltonian in a basis that is built up from this trial state. The basis is incremented one wavevector at a time by operating on the last basis state with the Hamiltonian and then orthonormalizing the product to all previous basis states. Notice, however, that by construction $H|i\rangle$ will have no overlap with states numbered *higher* than $|i+1\rangle$. Since the Hamiltonian is Hermitian, it must also be true that $H|i\rangle$ will have overlap with no state numbered *lower* than $|i-1\rangle$. In generating a new basis state, then, we need to orthogonalize $H|i\rangle$ against only two states, $|i\rangle$ and $|i-1\rangle$, in order to form $|i+1\rangle$, and hence the recursive procedure for generating basis states does not slow down as the basis set grows. To within roundoff errors, this approach maintains an orthogonal set of vectors.

Within this set of orthonormal vectors, that linear combination of states with the lowest expected energy forms a new estimate of the ground state. One finds this combination by diagonalizing the Hamiltonian, which is tridiagonal in this basis. The basis will probably not be complete: we generally will truncate it when we have run out of computer memory, when the estimate of the ground-state energy stops dropping, or when the residual of a new state, after orthogonalizing to other components, is negligible.

Representing the Hamiltonian in this recursively constructed basis has many advantages. First, the Hamiltonian will be tridiagonal and, so, very easy to study. More importantly, solutions for ground states and optical spectra do not require the generation of complete sets of states. For example, in working on half-filled twelve-site rings, the Hilbert space has nearly 10^6 dimensions. Formally, solutions would require complete bases, involving nearly 10^6 iterations of H acting on some $|v\rangle$ — not to mention the companion orthogonalizations and normalizations of these very large wavefunctions. Even if one worked in a subspace of high symmetry, a complete subbasis would entail, at the very least, many tens of thousands of such computations. In practice, however, one can estimate the ground-state wavefunction with high precision (say, ground-state energies to five decimal places) using only a few dozen basis states — even starting from a random trial vector. Computer memory requirements are limited to storing a relatively small number of wavefunctions.

Importantly, the calculations of optical absorption spectra — and hence also gaps, conductivities, and susceptibilities — are easily carried out by generating H in a suitable basis. For the optical absorption, which is our primary present interest, we first calculate the ground state, $|v_0\rangle$, using the technique described above. We then generate a new basis, using $J_q|v_0\rangle$ as the first state and obtaining subsequent states by the application of H . Once the basis has been generated, the problem

of calculating $\alpha(\omega)$ reduces to finding the spectral weight of this first state for the tridiagonal Hamiltonian. In essence, this amounts to determining the spectrum by measuring the moments of H^n and using the cumulant expansion. Again, convergence with the number of basis states is very good: typically, only a few dozen states are required. Even for a low-symmetry, large-space problem such as a soliton on an thirteen-site ring, fewer than 200 states are needed to achieve convergence of the spectrum to the eye. Some features of the spectra, such as the gap energy, can be determined to high precision with far smaller bases.

Given the size of the diagonalizations, the calculations are remarkably fast. To sweep a parameter range — say, a dozen different values of the dimerization — takes about twenty minutes on a CRAY supercomputer for a 12-site system. On the other hand, such a calculation requires several million words of computer memory and both the time and memory requirements grow by a factor of four for each additional site. Thus if one avoids the (slow) process of using external memory, the present limitation in system size is of order 14-15, even using the largest current computers. Though we do not report those measurements here, we have run up to 14-site lattices and could run 15-site chains on a CRAY 2 without incorporation of additional symmetries.

There are two points concerning the method which we should emphasize. First, we could clearly study somewhat (but not substantially) larger-sized systems by incorporating additional symmetries, such as restricting to a given *total* spin value (rather than just a specified value of S_z) or using mirror plane or other spatial symmetries. Indeed, a number of studies (see, e.g., ^{8,9}) using "valence bond diagrams" (see, e.g. ¹⁰) have examined specific properties of systems similar in size to ours on considerably smaller computers, by making extensive use of symmetries. However, apart from the question of simplicity, the virtue of using a code that does not depend on a particular spatial symmetry is that one can study ionic geometries in which this symmetry is not present. Thus for example, it is straightforward for us to study solitons, or the effects of e-e interactions on the phonon dispersion relation, simply by re-diagonalizing H in a different (and generally non-symmetric) ionic geometry.

Second, as we noted in the introduction, for (small) finite clusters with any given boundary conditions, the lattice-size dependence in numerical calculations is great. This is very familiar in the band theory limit (weak e-e interactions), in which the density of states for a finite-size lattice is a series of delta-function spikes at the k values allowed by the boundary conditions. Since the low-energy physics of the system depends on the states near the Fermi energy, this physics is highly dependent on whether such a spike lies on or near the Fermi surface or not.

A slightly different perspective on this strong finite size dependence provides an important hint as to how to improve the situation. In an infinitely deep but finitely wide square well potential the quantum energy levels are discrete, with spacing in energy determined by the width of the well. To use a well of a given width to mimic a wider well, with more closely spaced energy levels, we could "play" with the walls to randomize the phase every time the electron "interacts" with the wall. In the currently relevant case of a one-dimensional system (which we will (somewhat sloppily) refer to as a "chain"), the quantum phase of an electron travelling on the chain is well preserved if the chain is "soft". For ring boundary conditions, an electron, travelling around the ring, still "remembers" its phase after completing a full circuit. For open-ended chains, an electron, bouncing off the ends, builds up waves in the bulk. Thus, just as in the case of the energy levels in a square well, the quantum nature of these charge carriers leads to the marked sensitivity on size and boundaries.

For an infinite chain, of course, independent of the boundary conditions, an electron is not going to go away and come back with phase intact. To mimic this behavior

on finite chains, one can try as in the case of the square well to "randomize" the phase artificially; techniques to do this would include changing, as examples, a local hopping or an on-site energy or a Coulomb repulsion somewhere on the chain. Results from many such calculations could be averaged together to obtain a "phase-randomized" result. In the next section, we discuss this procedure in more detail and present evidence of its efficacy.

PHASE RANDOMIZATION

Although there has been some limited earlier work on using modified boundary conditions in the context of the Hubbard model^{3,4}, there is as yet no provably accurate prescription for randomizing the phase effectively for arbitrary U and V . The most obvious scheme is to change the complex phase of one of the hoppings on a closed ring^{3,4}. Physically, this corresponds to putting a magnetic flux through the ring and changes the locations of the momentum-space states. For $U = V = 0$, one can show, using arguments analogous to those used to prove Bloch's theorem, that this approach makes it possible to construct *exactly* larger units from smaller units by averaging over many different boundary conditions on the smaller units¹¹. In Fig. 1 we demonstrate this result. To be fair, in the case of dimerization versus U the best results, which are essentially indistinguishable from the infinite-chain limit over most of the range of U , come from second-order - i.e., $1/N$ and $1/N^2$ - extrapolations from results from finite chains which are constrained to have uniform dimerization. Nevertheless, Fig. 1 does show the promise of phase randomization. Again, we note that for this bond-phase/magnetic-flux scheme, the $U = 0$ limit is recovered exactly for every lattice size.

In general, however, in the absence of any provable prescription, one must rely on the following intuitive "rules" for choosing a randomization scheme. First, whatever change is made to randomize the phase must, of course, randomize the phase effectively. We will show that this seemingly obvious point is not content-free in our later discussion. Second, the change in the system: *must* be negligible as the lattice size is increased to infinity; for example, if only one bond or site is varied from calculation to calculation, then the effect of such a change is immaterial in the thermodynamic limit. Finally, the behavior for small lattice sizes must be illustrative of the infinite-size limit. Put another way, one must study results on various lattice sizes and still make some sort of extrapolation to the infinite chain.

Naively, it is possible to study the ground state but not to recover information about excited states using Lanczos methods. It is possible, however, to work within a manifold of different symmetry from the ground state to explore gaps of various symmetries. Further, it is also possible to study spectral distributions using the very same basis generation used to produce the ground state. One can produce and then operate on the ground state with, for example, the current operator to study the optical absorption. Then, starting with this new state, one can once again generate a basis in which the Hamiltonian is tridiagonal and study the spectral distribution of the optically-excited state in a truncated subspace. We shall discuss this approach and its results in the next section. Before proceeding, however, we should indicate both a difficulty that the optical absorption studies will pose for the bond-phase/magnetic-flux "randomizing" approach introduced above and the resolution of this difficulty by use of another, previously unstudied, phase randomization technique.

For the half-filled band systems we are currently considering, in the strongly correlated limit ($U \rightarrow \infty$ in eqn. (1)) every site in the ground state is singly occupied. The current operator (describing the absorption of a photon) creates excitonic com-

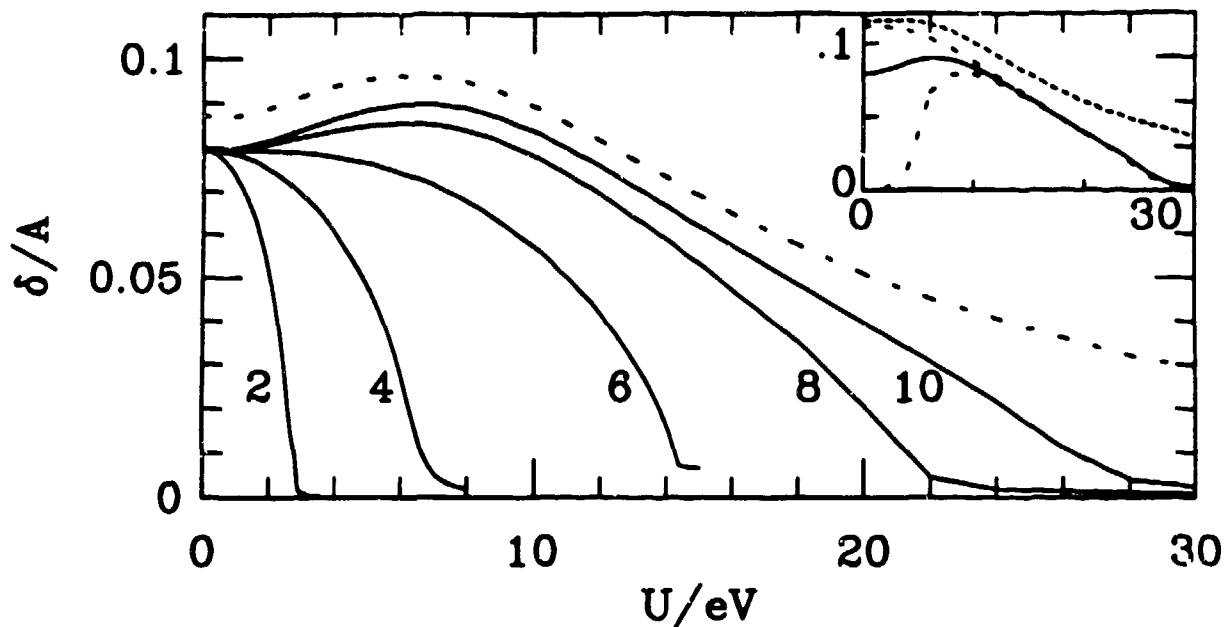


Fig. 1. Self-consistent dimerization (δ) as a function of Hubbard U for several N with $48/N$ different phase boundary conditions summed (solid lines) compared to the extrapolation to 48 sites from the chain constrained to have uniform dimerization (dashed line). Note the counter-intuitive increase of δ with U can be seen on systems as small as 8-sites. The phase-averaged result on 10 sites is compared in the inset with the 10-site chain (short-dashed) and 10-site ring with periodic or anti-periodic boundary conditions (dashed), where finite-size effects obscure this enhancement.

ponents - a double occupancy and a hole - each of which moves as a free particle over an effectively neutral background. Since these excitonic components are oppositely charged, they pick up opposite phases as they travel around the ring, through which we vary the magnetic flux. Thus, the effect of the flux is eliminated to lowest order and the bond-phase scheme becomes ineffective in the strong-coupling limit. To circumvent this difficulty, we shall instead multiply one of the hoppings by a real number x in the range $-1 \leq x \leq 1$. This affects the double occupancy and the hole equally and effectively randomizes electronic phase in the strong-coupling limit. Note that this approach clearly incorporates not only cases of the periodic ($x = 1$) and antiperiodic ($x = -1$) rings but also the case of the open chain ($x = 0$). Thus it is in accord with our comments about "filling in" the k -values in the Brillouin zone. As we shall see in the ensuing section, this "scaled-hopping" phase randomization technique produces results in good agreement with expectations based on both strong- and weak-coupling perturbation theory arguments.

RESULTS FOR OPTICAL ABSORPTION IN 1-D CORRELATED BANDS

The optical spectra of many novel solid-state materials provide crucial insights into both the relative strength of electron-phonon (e-p) versus electron-electron (e-e) interactions and the nature of the charge carriers. The case of the dominant e-p interactions has been widely studied in applications to quasi-one-dimensional conducting polymers. The classic example is the application of the Su-Schrieffer-Heeger (SSH) model¹⁰ to *trans*-(CH) _{n} . Here, the optical absorption spectrum of the ideally dimerized ground state exhibits a square-root singularity - characteristic of one-dimensional independent electron systems - at the edge of the optical gap. Further, the nonlinear

excitations — “kink” solitons, polarons, and bipolarons — produce clear signatures in the form of midgap absorptions with well-defined relative intensities (see, e.g.,¹¹ for a summary of these features). Conversely, motivated by potential applications to certain classes of charge-transfer salts¹⁴, the case of dominant e-e interactions has also been studied extensively^{7,15,16,17,18}, both within the Hartree-Fock approximation¹⁵ and using various strong-coupling approaches^{15,17,18} or diagonalization of small systems⁷. In this strong-coupling limit, the spectra — at least for weakly dimerized systems — are typically shifted to higher frequencies and do not exhibit the characteristic square-root singularity at the onset of absorption. Similarly, the characteristic midgap absorptions associated with the localized nonlinear excitations are also shifted substantially — and, in some cases, essentially removed¹⁹ — from their positions in the e-e interaction case.

In view of these substantial qualitative differences, it is hardly surprising that in the continuing debate about the relative strength of e-p versus e-e interactions in conducting polymers, considerable recent attention has focused on the optical absorption spectra. To go beyond the purely e-p models in the regime of weak e-e interactions, perturbation theory has been invoked^{19,20}, whereas for strong e-e interactions, leading-order estimates and qualitative arguments have been presented¹⁹. These analyses leave open the vital question of the characteristics of the optical absorption spectra for intermediate coupling, where the contributions of both the e-p and e-e interactions are expected to be significant and *a priori* neither interaction can be neglected or be treated in perturbation theory. Earlier studies in this intermediate-coupling regime, using valence-bond techniques to obtain (numerically) exact results for the full many-body problem on small finite systems^{21,22,23}, focused primarily on the value of the “optical gap” — more precisely, on the location of the first optically allowed 1B_u state — and on the two-photon allowed 2A_g state and did not attempt to study directly $\alpha(\omega)$, the optical absorption as a function of frequency. Our present Lanczos approach, coupled with the phase-randomization/boundary-condition-averaging technique allows us for the first time to produce high-resolution spectra on small systems.

To begin our discussion we recall the analytic forms for the optical absorption spectra that are available in a wide range of limiting cases. In the absence of electronic correlations, the Peierls-Hubbard model reduces to the SSH model. Here a number of analytic results are available, particularly if one works in the continuum limit, an approximation valid if, as is the case for *trans*-(CH)_{*n*}, the optical gap is small compared to the bandwidth and the excitations (e.g., solitons and polarons) extend over many lattice spacings. The uniform dimerization of the lattice caused by the e-p coupling opens up a gap between the valence and conduction bands, while defects in the uniform distortion appear as localized states in the gap. For the purely dimerized case¹³,

$$\alpha(\omega) \propto 1 / \omega^2 \sqrt{\omega^2 - \Delta^2} \quad . \quad (5)$$

where Δ is the gap energy. There is a characteristic square-root singularity at the gap edge due to the divergence in the density of states for transitions from the top of the valence band to the bottom of the conduction band. For the lattice model, the primary qualitative difference is that the absorption is cut off at the bandwidth $4t_0$ with another square-root singularity. Provided Δ is much less than $4t_0$, this difference is small, however, since it occurs at high energy, where all absorptions are attenuated by the $1/\omega^2$ factor due both to vanishing matrix elements and large energy denominators. For a soliton, transitions between the midgap state and one of the two bands give rise to a contribution of the form¹³

$$\alpha_s(\omega) \propto (\omega^2 - (\Delta/2)^2)^{-1/2} \times \text{sech}^2 \frac{\pi}{\Delta} (\omega^2 - (\Delta/2)^2)^{1/2} \quad . \quad (6)$$

while somewhat bleaching the interband spectrum. This midgap absorption has the same singular structure due, again, to the divergent density-of-states at the gap edge.

In the limit of large U (compared to t_0), the optical absorption is expected to be quite different. Since no two electrons, independent of spin, may occupy the same site, at half-filling, the sites are all "jammed", each has exactly one electron and none of the electrons may move. Indeed, in this limit one may prove to leading order in t_0/U the equivalence of the system to a completely filled (and therefore inert) band of *spinless* fermions²⁴. If, on the other hand, one electron is removed, then the resultant hole moves as a free particle against this packed background with the same energy $\epsilon_k = -2t_0\cos(k)$ as an electron moving in an otherwise empty band. Meanwhile, although adding an extra electron to the half-filled lattice costs the large energy U , once that energy has been paid, the double occupancy also moves as a free particle, with energy $U + \epsilon_k$. Starting with the fully filled background, then, the optical excitations create double occupancies and holes in pairs at a total energy $U + 2\epsilon_k$ relative to the ground state; hence the range of the absorption should be from $U - 4t_0 < \omega < U + 4t_0$. Longer-range Coulomb repulsions produce an *attractive* interaction between the double occupancy and the hole - the standard excitonic binding mechanism - and thus skew the absorption spectrum toward lower energies. If the system is dimerized, the Brillouin zone is halved, giving rise to $\pm\sqrt{\epsilon_k^2 + (\Delta/2)^2}$ bands for the hole and $U \pm \sqrt{\epsilon_k^2 + (\Delta/2)^2}$ bands for the double occupancy. The gap which opens up in the bands opens a companion gap around the line $\omega = U$ in the optical absorption. These arguments show us where allowable transitions may occur. More detailed calculations^{16,17,18}, which incorporate information about the density of states and transition matrix elements, are needed to determine the shape of the spectra.

We can obtain further insight by considering a different "solvable" situation. In the limit of large dimerization - which, for purposes of illustration, we assume to be *fixed*, i.e. *not* self-consistently determined as a function of U - the hopping integral on the long bonds vanishes exponentially. For the model Hamiltonian in eqn. (1), this overlap vanishes completely for dimerization δ_0 satisfying $t_0 - \alpha\delta_0 = 0$. In this "decoupled dimer" limit, the chain may be thought of as being composed of independent, two-site systems, each having two electrons with an enhanced hopping parameter $t' = t_0 + \alpha\delta$. Further, each two-site cell has only one optical transition, at energy $\omega = U/2 + \sqrt{(U/2)^2 + (2t')^2}$, which, in strong coupling, is the absorption $\omega = U$ described above.

Armed with these analytic results for the limiting cases of strong and weak coupling and the "decoupled dimers", we investigate the optical absorption using exact diagonalizations. Specifically, we operate in a real-space basis, expressing electronic wavefunctions as products of up-electron and down-electron wavefunctions. As noted above, the only space-reducing symmetry we use is S_z , which given the form of H is in practice equivalent to conservation of the number of, individually, up and down electrons. While incorporation of other symmetries would in practice reduce the size of the Hilbert space - and, consequently, of computer time and memory requirements - such incorporation would come at a great cost in the complexity of the computer code, and, more importantly, in the generality of problems, especially with regard to lattice distortions.

We have measured the optical gap as a function of Coulomb terms U and V and lattice distortion δ . Our computed values for the gap for U and δ agree with Soos and Ramesh²³ on both chains and rings to stated precision. (Actually, Soos and Ramesh simply measure the gap to the lowest excited state of the correct symmetry while we measure the lowest energy absorption. For doubly-even rings, there exists a low-lying state for which the matrix element for excitation from the ground state is

zero. Hence, for these rings these two definitions of the gap are not equivalent and produce different results.)

In Fig. 2, we plot the optical gap as a function of U . The gap was calculated on 8-, 10-, and 12-site chains and then extrapolated to the infinite-chain limit using $\Delta = a + b/N + c/N^2$. Chain geometries offer the best finite-size extrapolations since all even- N chains have single-particle states which straddle the fermi energy. In contrast, the structure of the single-particle density of states varies dramatically for even and odd rings. The solid lines in the figure are the infinite-chain extrapolations for dimerized lattice distortions $\delta_t = (-)^t \delta$ of amplitudes $\delta = 0.00\text{\AA}$, 0.07\AA , and 0.14\AA . The dashed lines are strong-coupling expressions for the gap to 0th, 1st, and 2nd order. Throughout, we will use the standard SSH parameter values for *trans*-(CH)_{*x*}: $t_0 = 2.5\text{eV}$, $a = 4.1\text{eV}/\text{\AA}$, and, though it does not enter here, $K = 21\text{eV}/\text{\AA}^2$. Numerically differentiating the gap energy with respect to dimerization, we find that the increase of the gap due to dimerization is greatest for intermediate couplings $U \approx 4t_0 = 10\text{eV}$. All the same, even for intermediate couplings, the gap is already dominated by the contribution from e-e interactions rather than by that from the lattice distortion.

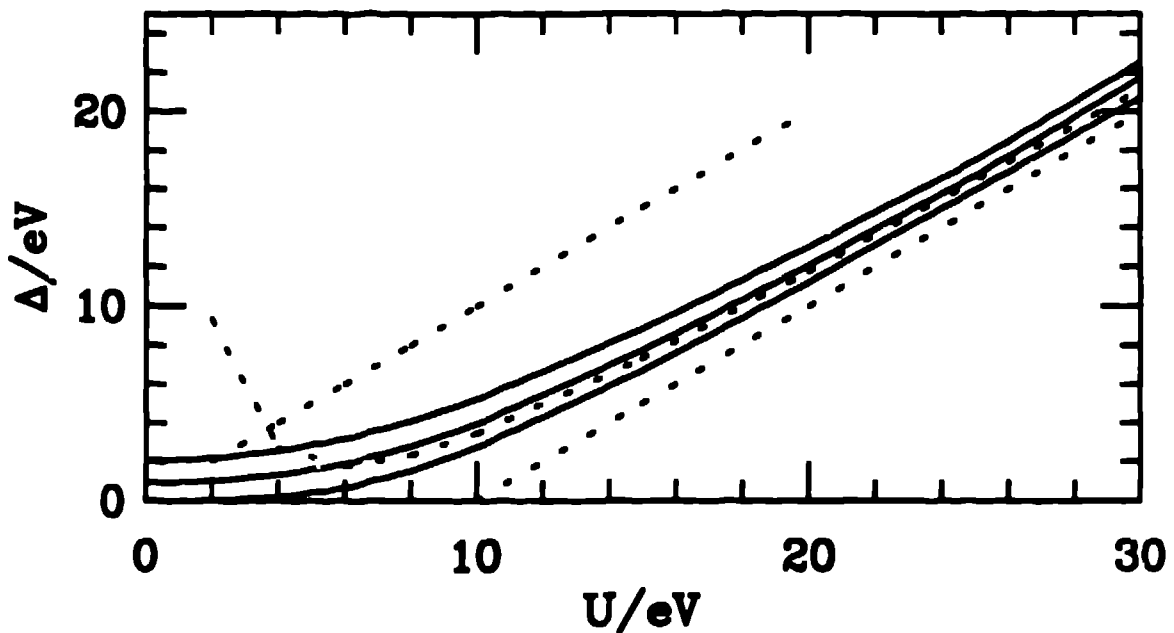


Fig. 2 Optical gap as a function of Hubbard U , extrapolated to infinite chains. The three solid lines are for $\delta = 0.00\text{\AA}$, 0.07\AA , and 0.14\AA , respectively. The dashed lines are the strong-coupling expansions to 0th, 1st, and 2nd order.

We have also measured the optical gap as a function of nearest-neighbor repulsion V , using 8-, 10-, and 12-site chains and extrapolating to infinite chains. While V lowers the gap for the finite chains, the extrapolated result is remarkably flat in strong coupling. To understand this result we recall our earlier remark that the effect of off-site Coulomb interactions is to provide an attraction between the double occupancy (charge e^-) and the hole (charge e^+) created in the optically excited state¹⁷. This attraction lowers the expectation value of the energy of that state and hence skews the absorption spectrum to lower energy. The current operator has odd parity, however, and thus a weak attraction will not be sufficient to bind the excitonic components (the double occupancy and the hole) in the optically excited state. In particular, if the lowest-energy component of the state is unbound, the double occupancy and the hole will be delocalized and the ability of the electrostatic attraction between them to decrease the gap energy will vanish with chain length. Thus we conclude that the

gap will decrease with V as $N \rightarrow \infty$ only when the off-site Coulomb force is strong enough to bind the exciton.

The most difficult aspect in measuring spectra is the sparseness of the spectral peaks for finite-size systems. Clearly, there will only be a limited number of transitions for a finite-size system. One might imagine that, since the number of states in the system grows exponentially with the number, N , of spatial sites, the finite sampling of the infinite-ring spectrum presents no great difficulties. In fact, however, the number of significant transitions typically grows only linearly with N . In the limit of weak electronic correlations, for example, the electrons are essentially noninteracting and the optical transitions can be described in terms of the N different single-particle energy levels. Meanwhile, when the Hubbard U is very large, the electrons essentially become noninteracting, spinless fermions, whose transitions, again, are characterized by N different energies. Further, even in intermediate coupling ($U = 10\text{eV}$) and on fairly large ($N = 12$) rings, one gets only four absorption peaks for periodic boundary conditions for the dimerized lattice. Clearly all this depends on the symmetry of the lattice distortion as well as on the strength of the electronic interactions. In highly asymmetrical cases the *non-randomized* spectra may have reasonable numbers of peaks. However, in these asymmetric cases it is typically difficult to distill the essential physics from the spectra. In sum, we find that for any fixed set of boundary conditions the optical spectra are sampled in a (disappointingly!) sparse manner over the entire range of electronic correlations: said another way, finite-size effects appear in a decidedly quantum fashion in the absorption spectra.

We have already indicated that "phase randomization techniques" can help us resolve this problem and further given some qualitative arguments about what to expect. In Fig. 3 we show plots of phase-randomized spectrum – using the "bond phase/ magnetic flux" method ^{3,4} discussed in the previous section – for two values of U in the weak coupling regime : $U = 1\text{eV}$ and $U = 4\text{eV}$, with the bandwidth taken to be $4t_0 = 10\text{eV}$. Note that in the Fig. 3 we have already "smoothed" the δ -function spikes by replacing them by Lorentzians of width 0.5eV to produce a continuous spectrum. While the $U = 1\text{eV}$ curve (the lower, smoother one) is reasonable, the $U = 4\text{eV}$ curve is starting to show signs of fairly sparse structure, despite the Lorentzian smoothing. This indicates the breakdown, anticipated in our earlier discussion, of the "magnetic flux/bond phase" randomization scheme.

To transcend the limitations of this "bond phase/magnetic flux" approach, we have adopted the "scaled hopping" procedure discussed in the previous section and have randomized the phase by averaging the different spectra that are found by varying the magnitude of the "boundary" hopping –i.e., between sites 1 and N – from $-(t_0 - \alpha\delta_N)$ to $+(t_0 - \alpha\delta_N)$ in ten equal steps. Again we smooth the spectrum by replacing the δ -function spikes by Lorentzians of width 0.5eV .

In Fig. 4, we show the phase-randomized spectra produced by this technique for electrons on a 12-site ring in the strongly interacting case with $U = 30\text{eV}$ for both a uniform lattice ($\delta = 0$, solid line) and for a strongly distorted lattice ($\delta = 0.14\text{\AA}$, dashed line). The gross features of the spectra are predicted by strong-coupling calculations ^{16,18}. The numerical spectra, however, show substantially more interesting detail. The optical absorption, which to first order in the hopping is rounded, symmetric, and extends from $U - 4t_0$ to $U + 4t_0$, is shifted to higher energies in higher order. It is still centered about $\omega = U$ and so becomes skewed for finite U . In particular, the absorption has a fairly sharp onset at the gap while at high energies $\alpha(\omega)$ vanishes with a finite slope. In the presence of a strong dimerization, the gap is enhanced slightly and a strong absorption appears at $U/2 + \sqrt{(U/2)^2 + (2t')^2} = 31.2\text{eV}$, as predicted by the decoupled-dimer argument. The peak due to the dimerization is decidedly asym-

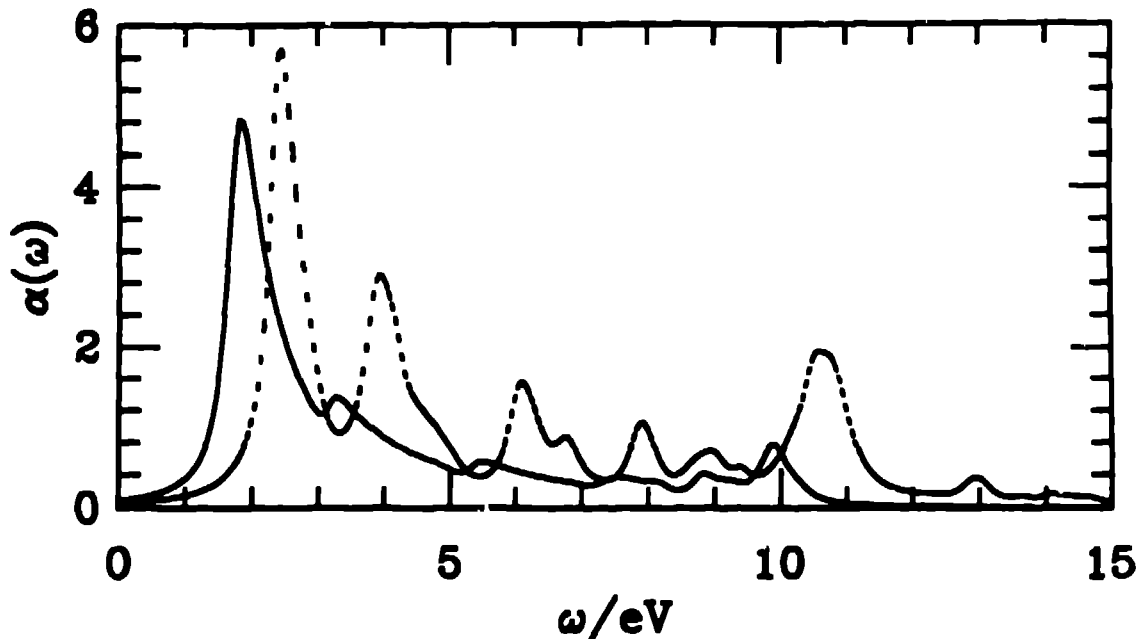


Fig. 3. The optical absorption spectra calculated using the "bond phase/magnetic flux" phase randomization method for $U = 1\text{eV}$ (lower smoother curve) and for $U = 4\text{eV}$ (upper, more jagged curve) for the case in which the full band width $4t_0 = 10\text{eV}$. Note the "sparseness" of the spectrum in the latter case.

metric, with, again, a sharp onset on the low-energy side. The undimerized absorption is noticeably depleted on the high-energy side of the absorption peak, corresponding to the gap which opens up in the strong-coupling absorption¹⁸ due to the gaps in the single-particle bands. There may be a companion depletion on the low-energy side, but it appears to disappear with increasing ring size.

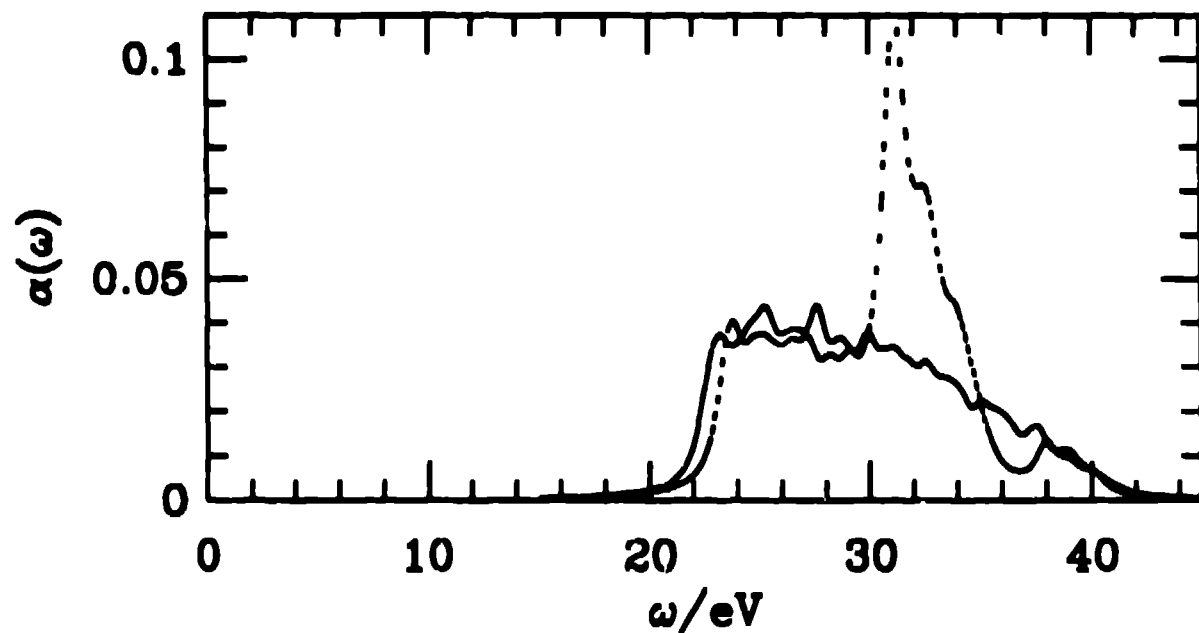


Fig. 4. The phase randomized optical spectra obtained using the "scaled hopping" approach described in the text for 12-site rings at strong coupling ($U = 30\text{eV}$). The solid and dashed lines are for the uniform and dimerized ($\delta = 0.14\text{\AA}$) lattices, respectively.

For intermediate coupling $U = 4t_0 = 10\text{eV}$, Fig. 5 shows phase-randomized spectra for a uniform lattice ($\delta = 0$, solid line) and for a strongly distorted lattice ($\delta = 0.14\text{\AA}$, dashed line) of 12 sites. The scale of $\alpha(\omega)$, of course, is greater than in the case of stronger coupling shown in Fig. 4, as one would predict from the f-sum rule^{7,25,26}.

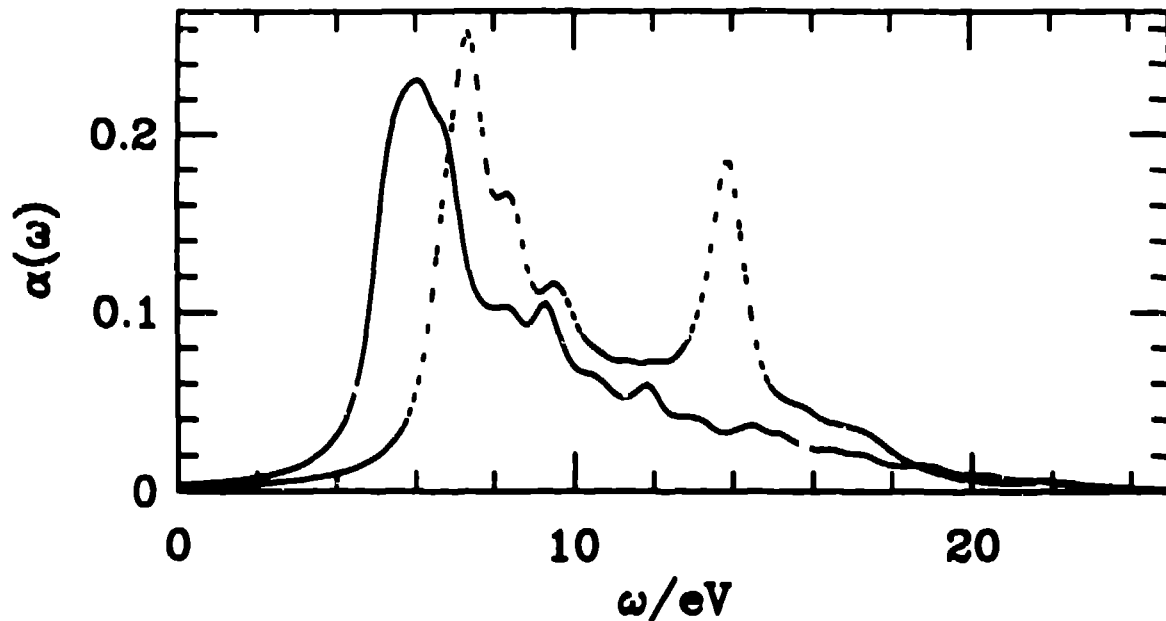


Fig. 5 The phase randomized optical spectra obtained using the "scaled-hopping" approach described in the text for 12-site rings at intermediate coupling ($U = 10\text{eV}$). The solid and dashed lines are for the uniform and dimerized ($\delta = 0.14\text{\AA}$) lattices, respectively.

The results in Fig. 5 are truly hybrids of the weak- and strong-coupling absorptions. The undimerized spectrum might be thought of as strong-coupling absorption¹⁶ — as in Fig. 4 — which has been strongly skewed to the low-energy side, as we would expect from the small value of U . A more natural picture, however, might be to associate the gap-edge peak with the square-root singularity from the diverging density-of-states, as in the noninteracting case, despite the fairly substantial value of U . Despite this interpretation, we should stress that, as a comparison of the two curves in Fig. 5 demonstrates, the gap is due mostly to e-e interactions. The dimerization raises the gap somewhat — more here, in any case, than for the $U = 30\text{eV}$ case shown in Fig. 4 — but its principal effect is to give rise to a "decoupled-dimer" peak, characteristic of strong coupling. If we were to plot spectra for strongly distorted lattices over a wide range of U , all on the same plot, we would observe two envelopes. One envelope would trace out the decoupled-dimer peak, pronounced at large U and swallowed up at small U by the weak-coupling absorption. Conversely, the other envelope, corresponding to the density-of-states peak, would dominate at small U , but then disappear under the decoupled-dimer peak at higher energies. In intermediate coupling, both structures are comparable. Notice, finally, that, apart from a slight, familiar depletion on the high-energy side of the peak, in Fig. 5 the decoupled-dimer peak appears not to bleach the undimerized spectrum but simply to increase the integrated weight of the spectrum. This is related by the f-sum rule^{7,25,26} to the increase in the magnitude of the delocalization energy as the dimerization gap is opened up.

We have also investigated the effect of a nearest neighbor V on the absorption

spectrum. At half-filling, the effect in strong coupling of V on the ground state is almost exactly to reduce the effective value of U to $U - V$. For optical spectra, V only qualitatively reduces the effective value of U . As noted earlier, V is somewhat ineffectual in reducing the gap energy until it is strong enough to bind the optically excited exciton. On the other hand, the centroid of the spectrum, which we define as $\int \omega^2 \alpha(\omega) / \int \omega \alpha(\omega)$, is quite nearly equal to $U - V$. Hence, V skews the absorption toward lower energies, much as for a reduced U . Turning on V is also like a reduced U in that V suppresses the decoupled-dimer peak.

Finally, Fig. 6 shows the absorption of a neutral and of a charged *soliton* on a 11-site ring. Phase randomization has not been used to produce these spectra in part because the reduced symmetry of the problem gives richer structure but mainly because we have been unable to find a scheme which effectively randomizes electronic phases while locking the "midgap" state at midgap. As a consequence, the figure is not extremely illuminating. It does serve to show, as discussed in a number of articles, that the effect of an intermediate $U = 4t_0 = 10\text{eV}$ is to shift the charged midgap absorption (dashed line) to lower energy while shifting the neutral soliton (solid line) to higher ω , where it blends into the intergap absorption.

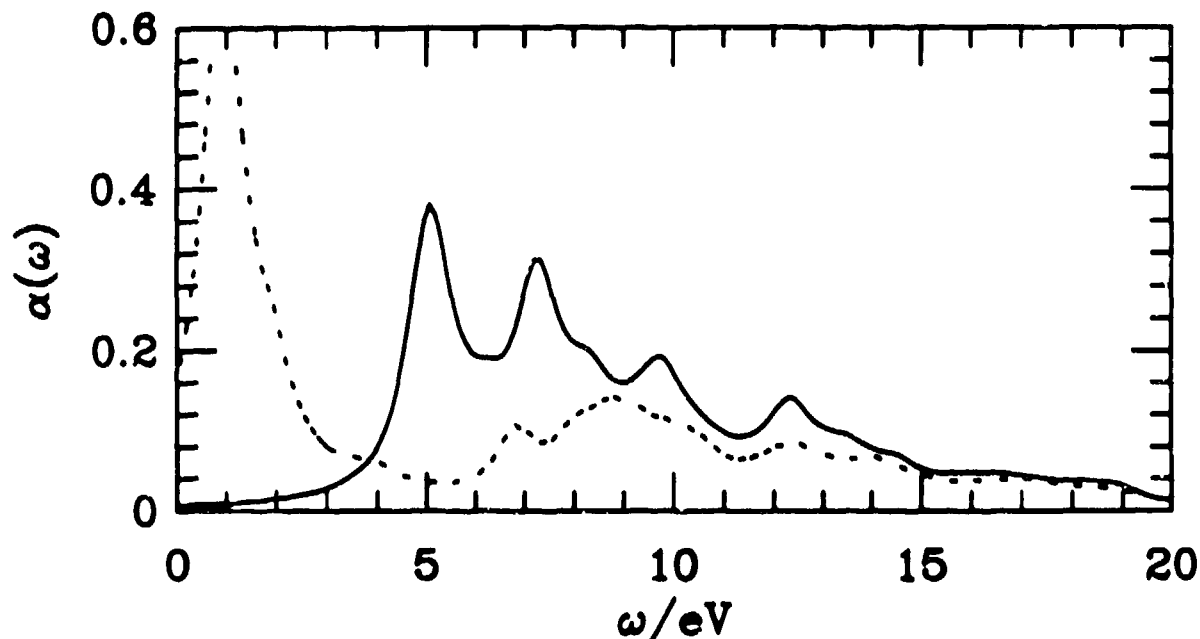


Fig. 6 The optical spectra for 11-site rings at intermediate coupling ($U = 10\text{eV}$). The solid and dashed lines are for the uniform and dimerized ($\delta = 0.14\text{\AA}$) lattices, respectively.

CONCLUSIONS AND OPEN ISSUES

We believe that our results establish that the combination of Lanczos exact diagonalizations with phase randomization techniques can be used to obtain insight into many properties of strongly interacting electron systems from studies of (even small) finite size systems.

In the case of optical absorption spectra, since electron phases interfere quantum mechanically over the entire extent of small rings or chains, small systems are strongly discrete and have very sparse spectra. Phase randomization is essential to produce high resolution spectra from exact diagonalizations on these small (up to 12 site) rings. Simple results from limits of strong and weak electronic correlations and of large

lattice distortions help us to understand results in the difficult intermediate-coupling regime. In the limit of infinite U , half-filled rings show wide, rounded absorption spectra centered about $\omega = U$. As U is decreased or V is turned on, this structure is skewed toward lower energies. In the limit of vanishing U , the skewed absorption turns into a peak at the gap edge as a square-root divergence develops in the density-of-states. For infinite U , dimerization introduces a strong peak, corresponding to the limit of decoupled two-site dimers, in the middle of the absorption. Dimerization opens up gaps in the single-particle bands and so should also open up gaps in the optical absorption around the decoupled-dimer peak. In finite U , the decoupled-dimer peak is suppressed and the gaps in the absorption are somewhat washed out, particularly on the low-energy side of the peak. In weak coupling, there are neutral- and charged-soliton absorptions at midgap. For finite U , the neutral-soliton absorption is shifted to higher energies while the charged-soliton midgap peak moves to lower ω .

Clearly much work remains. In particular, we have begun to perform these diagonalizations in momentum space to gain full control of electronic phase randomization. Our analyses of solitons and other localized defects are very preliminary, and one could indeed argue that since both our phase randomization technique and these intrinsic defects can be viewed as $1/N$ effects, it may prove very difficult to extract more reliable information about solitons than is already available. However, we hope to be able to incorporate our knowledge of important physical features — e.g., midgap states — of one-dimensional electron-phonon models to a greater extent in calculating high-resolution spectra in the presence of difficult excitations, such as solitons and polarons.

ACKNOWLEDGEMENTS

We would like to thank Sumit Mazumdar, Doug Scalapino, and Zoltan Soos for several valuable discussions and Michael Ziegler for bringing references 3 and 4 to our attention. Computational support was provided by the Centers for Materials Science and Nonlinear Studies at Los Alamos National Laboratory, by the Computational Sciences Division of the U.S. DOE at the NMFECC at Livermore, and by the DOE's Supercomputing Access Program at the Air Force Supercomputer Center.

REFERENCES

- 1 See, e.g., the section on Lanczos diagonalization in S. Pissanetsky, Sparse Matrix Technology, London: Orlando, Academic, 1984.
- 2 For an early study of the application of the Lanczos method to the pure Hubbard model, see B. Fourcade and G. Spronken, Phys. Rev. B **29** (1984) 5012.
- 3 R. Julien and R. M. Martin, Phys. Rev. B **26** (1982) 6173.
- 4 A. M. Oles, G. Tréglia, D. Spanjaard, and R. Julien, Phys. Rev. B **32** 2167.
- 5 Recent studies of the extended Peierls-Hubbard models include: S. Mazumdar and S.N. Dixit, Phys. Rev. Lett. **51** (1983) 292 and Phys. Rev. B **29** (1984) 1824; J.E. Hirsch, Phys. Rev. Lett. **51** (1983) 296; Z.G. Soos and S. Kanamashu, *ibid.* **51** (1983) 2374; D. K. Campbell, T. A. DeGrand, and S. Mazumdar, *ibid.* **52** (1984) 1717; J. E. Hirsch and M. Grabowski, *ibid.* **52** (1984) 1713; W.K. Wu and S. Kivelson, Phys. Rev. B **33** (1986) 8546; S. Kivelson and W.K. Wu, *ibid.* **34** (1986) 5423; S. Kivelson and D.E. Renn, *ibid.* **26** (1982) 4278.
- 6 W.P. Su, J.R. Schrieffer, and A.J. Heeger, Phys. Rev. Lett. **42** (1979) 1698; Phys. Rev. B **22** (1980) 2099
- 7 P. F. Maldague, Phys. Rev. B **16** (1977) 2437

8 S. Ramasesha and Z. G. Soos, J. Chem. Phys. **80** (1984) 3278.
9 S. Mazumdar and S. N. Dixit, Synth. Met. **28** (1989) 463.
10 S. Mazumdar and Z. G. Soos, Synth. Met. **1** (1979) 77.
11 D.K. Campbell, J.T. Gammel, and E. Y. Loh, Jr., in preparation.
12 V. Waas, J. Voit, and Hüttner, Synth. Met. **27** (1988) A21.
13 K. Fesser, A. R. Bishop, and D. K. Campbell, Phys. Rev. B **27** (1983) 4804.
14 J. B. Torrance, B. A. Scott, and D. B. Kaufman, Sol. State Comm. **17** (1975) 1369.
15 K. Kubo, J. Phys. Soc. Japan **31** (1970) 30. Sol. St. Comm. **17**, (1975) 1369.
16 S. K. Lyo and J.-P. Gallinar, J. Phys. C. **10** (1977) 1693.
17 S. K. Lyo, Phys. Rev. B **18** (1978) 1854.
18 J.-P. Gallinar, J. Phys. C. **12** (1979) L335.
19 D. K. Campbell, D. Baeriswyl, and S. Mazumdar, Physica **143B** (1986) 533; Synth. Metals, **17** (1987) 197.
20 W.-K. Wu and S. Kivelson, Phys. Rev. B **33** (1986) 8546.
21 S. R. Bondeson and Z. G. Soos, Chem. Phys. **44** (1979) 403.
22 S. Mazumdar and Z. G. Soos, Phys. Rev. B **23** (1981) 2810.
23 Z. G. Soos and S. Ramasesha, Phys. Rev. B **29** (1984) 5410.
24 J. Bernasconi, M.J. Rice, W.R. Schneider, and S. Strässler, Phys. Rev. B **12** (1975) 1090.
25 D. Baeriswyl, J. Carmelo, and A. Luther, Phys. Rev. B **33** (1986) 7247; **34** (1986) 8976(E).
26 S. Kivelson, T.-K. Lee, Y.-R. Lin-Liu, I. Peschel, and L. Yu, Phys. Rev. B **25** (1982) 4173.